Neuron
Article

Microglia Sculpt Postnatal Neural Circuits in an Activity and Complement-Dependent Manner

Dorothy P. Schafer,[1] Emily K. Lehrman,[1,5] Amanda G. Kautzman,[1,5] Ryuta Koyama,[1] Alan R. Mardinly,[3] Ryo Yamasaki,[4] Richard M. Ransohoff,[4] Michael E. Greenberg,[3] Ben A. Barres,[2] and Beth Stevens[1,*]
[1]Department of Neurology, F.M. Kirby Neurobiology Center, Children's Hospital, Harvard Medical School, Boston, MA 02115, USA
[2]Department of Neurobiology, Stanford University School of Medicine, Stanford, CA 94305, USA
[3]Department of Neurobiology, Harvard Medical School, Boston, MA 02115, USA
[4]Neuroinflammation Research Center, Department of Neurosciences, Lerner Research Institute, and Mellen Center for MS Treatment and Research, Neurological Institute, Cleveland Clinic, Cleveland, OH 44195, USA
[5]These authors contributed equally to this work
*Correspondence: beth.stevens@childrens.harvard.edu
DOI 10.1016/j.neuron.2012.03.026

SUMMARY

Microglia are the resident CNS immune cells and active surveyors of the extracellular environment. While past work has focused on the role of these cells during disease, recent imaging studies reveal dynamic interactions between microglia and synaptic elements in the healthy brain. Despite these intriguing observations, the precise function of microglia at remodeling synapses and the mechanisms that underlie microglia-synapse interactions remain elusive. In the current study, we demonstrate a role for microglia in activity-dependent synaptic pruning in the postnatal retinogeniculate system. We show that microglia engulf presynaptic inputs during peak retinogeniculate pruning and that engulfment is dependent upon neural activity and the microglia-specific phagocytic signaling pathway, complement receptor 3(CR3)/C3. Furthermore, disrupting microglia-specific CR3/C3 signaling resulted in sustained deficits in synaptic connectivity. These results define a role for microglia during postnatal development and identify underlying mechanisms by which microglia engulf and remodel developing synapses.

INTRODUCTION

Early in development neurons make far more synaptic connections than are maintained in the mature brain. Synaptic pruning is an activity-dependent developmental program in which a large number of synapses that form in early development are eliminated while a subset of synapses are maintained and strengthened (Hua and Smith, 2004; Katz and Shatz, 1996; Sanes and Lichtman, 1999). While it is clear that neuronal activity plays a role, the precise cellular and molecular mechanisms underlying this developmental process remain to be elucidated.

Microglia are the resident CNS immune cells which have long been recognized as rapid responders to injury and disease, playing a role in a broad range of processes such as tissue inflammation and clearance of cellular debris (Hanisch and Kettenmann, 2007; Kreutzberg, 1996; Ransohoff and Perry, 2009). In contrast to disease pathology, the function of microglia in the normal, healthy brain is far less understood. However, recent studies suggest that microglia may play a role in synaptic remodeling and plasticity in the healthy brain (Davalos et al., 2005; Nimmerjahn et al., 2005; Paolicelli et al., 2011; Schafer et al., 2012; Tremblay et al., 2010a; Wake et al., 2009). For example, microglia within the juvenile visual cortex modify their association with dendritic spines in response to changes in visual sensory experience (Tremblay et al., 2010a). A more recent study provides evidence that disruptions in microglia function result in delayed maturation of hippocampal synaptic circuits (Paolicelli et al., 2011). Moreover, data from these studies suggest that microglia may be phagocytosing dendritic spines. These intriguing studies raise several interesting and important questions. The precise function of microglia at synaptic sites, the molecular mechanism(s) underlying microglia-mediated synaptic engulfment, and the long term consequence(s) of disrupting microglia function on synaptic circuits remain a mystery.

A candidate mechanism by which microglia could be interacting with developing synapses is the classical complement cascade. Complement cascade components C1q and C3 localize to immature synapses and are necessary for the developmental pruning of retinogeniculate synapses (Stevens et al., 2007; Stephan et al., 2012). While provocative, the mechanism by which complement mediates synaptic pruning has remained completely unknown. Complement components function in the immune system by binding and targeting unwanted cells and cellular debris for rapid elimination through several different pathways. Among the many mechanisms by which complement may mediate synaptic pruning is phagocytosis, which makes microglia, the resident CNS phagocyte, a candidate.

Given the questions that have now emerged regarding the role of microglia at CNS synapses, we sought to address precisely how microglia are interacting with developing synaptic circuits and determine the long-term consequences of disrupting microglia function on neural circuit development. In the current study, we demonstrate that microglia engulf presynaptic retinal inputs undergoing synaptic pruning in the postnatal brain and

determine that this process is regulated by neuronal activity. Furthermore, we identify signaling through a phagocytic receptor, complement receptor 3 (CR3/CD11b-CD18/Mac-1), expressed on the surface of microglia and its ligand, complement component C3, localized to synaptically enriched regions, as a key molecular mechanism underlying engulfment of developing synapses. Importantly, disruption of CR3/C3 signaling was specific to microglia in the CNS and resulted in sustained deficits in brain wiring. Taken together, these observations provide a role for microglia in the healthy, developing brain and provide a cellular and molecular mechanism by which microglia are physically interacting with synaptic elements.

RESULTS

Microglia Engulf RGC Inputs during a Period of Active Synaptic Pruning

To investigate the functional role of microglia in developmental synaptic remodeling, we used the mouse retinogeniculate system, a classic model for studying activity-dependent developmental synaptic pruning (Feller, 1999; Huberman et al., 2008; Shatz and Kirkwood, 1984). Early in development, retinal ganglion cells (RGCs) form exuberant synaptic connections with relay neurons throughout the dorsal lateral geniculate nucleus (dLGN) of the thalamus. During the pruning period, RGC synaptic inputs originating from the same eye as well as between eyes compete for territory throughout the dLGN (Chen and Regehr, 2000; Hooks and Chen, 2006; Jaubert-Miazza et al., 2005; Ziburkus and Guido, 2006). Spontaneous retinal activity plays critical role in this refinement process; however, the underlying cellular and molecular mechanisms remain poorly understood. (Del Rio and Feller, 2006; Feller, 1999; Penn et al., 1998; Shatz, 1990; Torborg and Feller, 2005).

During this robust pruning period (P5 in mouse), we used high resolution confocal imaging to assess the interactions between microglia and synaptic inputs throughout the dLGN. Contralateral and ipsilateral presynaptic inputs from RGCs were visualized in the dLGN by intraocular injection of anterograde tracers, cholera toxin β subunit conjugated to Alexa 594 (CTB-594) and Alexa 647 (CTB-647), respectively (Figure 1A). Microglia were labeled using the CX3CR1+/GFP mouse line in which all microglia express EGFP under the control of fractalkine receptor, CX3CR1, expression (Figure 1 and see Figures S1 and S5 available online; Cardona et al., 2006; Jung et al., 2000; Saederup et al., 2010).

At an age consistent with robust synaptic pruning (P5), microglial processes were in close association with RGC presynaptic inputs (Figure 1B and S2A). Upon closer examination, we detected numerous fluorescently labeled RGC inputs within the processes and soma of microglia (Figure 1B; Movies S1 and S2). Internalization was further confirmed by assessing confocal z stacks through individual microglia (Movie S2). This specific example is a microglia sampled from a region containing similar densities of overlapping ipsilateral (blue) and contralateral (red) RGC inputs (Figure 1A) which are undergoing active synaptic remodeling to establish nonoverlapping eye-specific territories (Figure 2A; Godement et al., 1984; Guido, 2008; Huberman et al., 2008; Sretavan and Shatz, 1986; Ziburkus and Guido, 2006). Consistent with simultaneous pruning of inputs from both eyes, contralateral (red) and ipsilateral (blue) RGC inputs were engulfed and localized within the microglia (Figure 1B; Movies S1 and S2). In addition, consistent with widespread pruning of RGC inputs throughout the P5 dLGN, we observed engulfment of RGC inputs in all synaptic regions (monocular and binocular). These data suggest that microglia engulf RGC inputs undergoing active synaptic remodeling.

To confirm that inputs are phagocytosed by microglia, RGC inputs from both eyes were labeled with CTB-594 and colocalization with CD68, a marker of lysosomes specific to microglia, was assessed in P5 dLGN. As suggested by previous dye-labeling experiments, the majority of engulfed RGC inputs were completely colocalized within lysosomal compartments (Figures 1C–1E). There were rare instances in which engulfed RGC inputs did not colocalize (Figures 1Ciii and 1E), and we suspect that these inputs are either in the process of being phagocytosed or are in phagosomal or endosomal compartments prior to lysosomal degradation. To further validate that microglia phagocytose RGC inputs, pHrodo-dextran, an anterograde tracer and pH-sensitive dye, was used to label RGC inputs (Figures S1A and S1B; Deriy et al., 2009; Miksa et al., 2009). Because pHrodo only fluoresces once it enters acidic compartments of lysosomes, any pHrodo-positive fluorescence within a microglia confirms phagocytosis of RGC inputs. Similar to previous experiments, pHrodo-positive RGC inputs were localized within microglia (Figures S1A and S1B). Furthermore, in addition to anterograde tracing with CTB and pHrodo, RGC input engulfment was also assessed within the P5 dLGN using a genetic approach, double transgenic mice expressing tdTomato under the control of Chx10, a transcription factor expressed by RGCs (Chx10-cre/Rosa26-STOP-tdTomato) (Figures S1C–S1F). Similar to CTB experiments, we observed tdTomato-labeled RGC inputs within lysosomal compartments of microglia. Importantly, these experiments exclude the possibility that engulfment is due to injury secondary to ocular injections. Together, we demonstrate that microglia phagocytose RGC inputs during a peak period of synaptic pruning in the dLGN.

Microglia-Mediated Engulfment of RGC Inputs Is Developmentally Regulated

To begin to address whether microglia-mediated engulfment of RGC inputs contributes to the normal process of synaptic pruning, we assessed the developmental regulation of microglia phagocytic capacity. We first characterized microglia activation state through development and observed a unique class of microglia in the early postnatal dLGN as compared to older ages (P30) (Figure S2). Microglia within the early postnatal dLGN had characteristic features of more ''activated'' cells traditionally associated with disease including increased phagocytic capacity (assessed by morphology and CD68 immunoreactivity; Figures S2C and S2D). Interestingly, early postnatal microglia also had processes, a morphological characteristic of 'resting' microglia which are resident in the healthy adult brain (Figure S2B; Lynch, 2009; Ransohoff and Perry, 2009).

To address whether engulfment of RGC inputs was developmentally regulated, we developed an in vivo phagocytosis assay

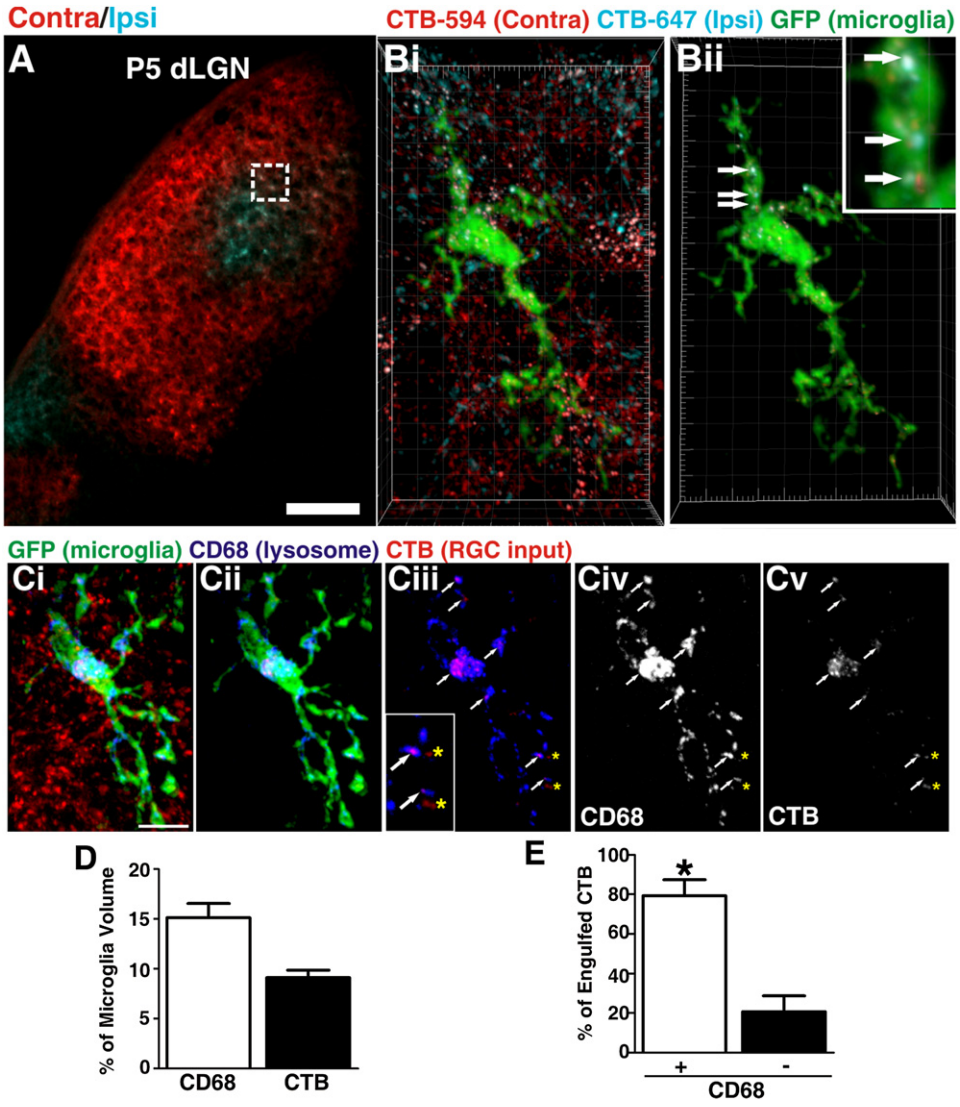

Figure 1. Microglia Engulf RGC Inputs Undergoing Active Synaptic Pruning in the dLGN

(A) A representative low-magnification image of P5 dLGN. Ipsilateral inputs are labeled with CTB-647 (blue) and contralateral inputs are labeled with CTB-594 (red). Scale bar = 100 μm.

(Bi) A microglia (EGFP, green) sampled from the border region of ipsilateral (blue) and contralateral (red) projections (inset in A). (Bii) All CTB fluorescence outside the microglial volume has been subtracted revealing RGC inputs (red and blue) that have been engulfed (arrows, enlarged in inset). Grid line increments = 5 μm.

(Ci) A representative microglia (green, EGFP) from P5 dLGN. RGC inputs from both eyes are labeled with CTB-594 (red) and lysosomes are labeled with anti-CD68 (blue). (Cii) The same microglia in which all CTB fluorescence outside the microglia volume has been removed revealing lysosomes (blue) and engulfed RGC inputs (red). (Ciii) The same cell in which only the lysosomes (blue) and RGC inputs (red) are visualized in which most inputs (red) are localized within CD68-positive lysosomes (blue; white arrows). There are few instances in which CTB is not localized to lysosomes (yellow asterisks). Inset is enlarged region of (Ciii). (Civ and Cv) The CD68 (Civ) and CTB (Cv) channels alone. Scale bar = 10 μm.

(D) Quantification of % volume of microglia occupied by CD68-positive lysosomes (white bar) and RGC inputs (black bar), n = 3 P5 mice.

(E) There are significantly more engulfed inputs localized to lysosomal compartments (white bars) versus nonlysosomal compartments (black bars). *$p < 0.001$ by Student's t test, n = 3 P5 mice.

All error bars represent SEM. See also Figure S1 and Movies S1 and S2.

(Figure 2A). Using high-resolution confocal microscopy followed by 3D reconstruction and surface rendering (Figure 2D), internalization of ipsilateral (CTB-647; blue) and contralateral (CTB-594; red) RGC inputs was quantified within the volume of each microglia (CX3CR1+/EGFP) throughout the dLGN. To control for variation in microglia volume, the following calculation was used: % Engulfment = Volume of internalized RGC inputs (μm^3)/Volume of microglia (μm^3). Consistent with microglial involvement in normal developmental synaptic pruning, engulfment of RGC inputs was developmentally regulated. During a developmental period of

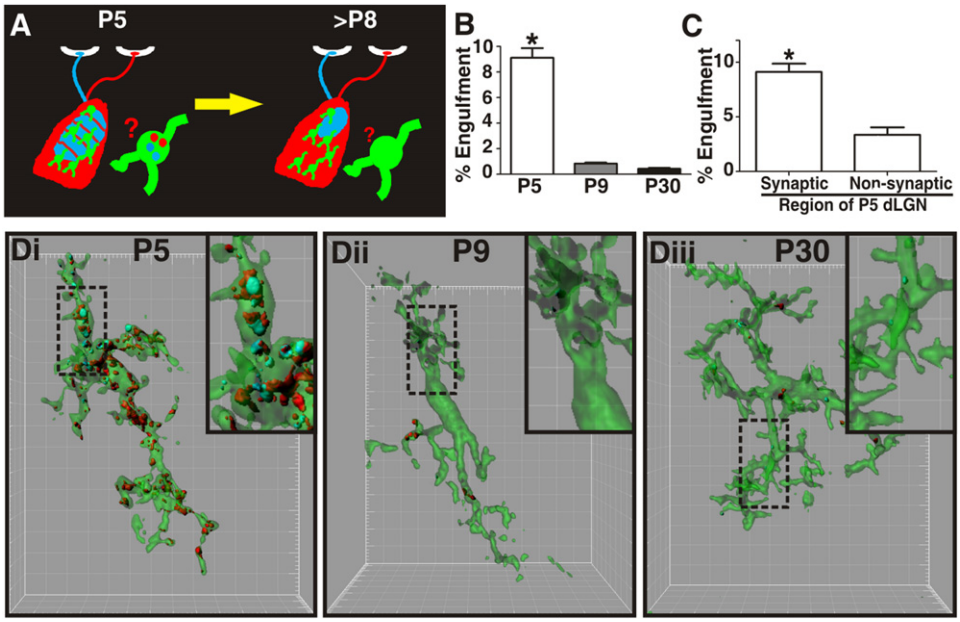

Figure 2. Microglia-Mediated Engulfment of RGC Inputs Is Developmentally Regulated

(A) Schematic of retinogeniculate pruning and strategy used for assessing engulfment. Contralateral (red) and ipsilateral (blue) inputs overlap at early postnatal ages (P5). Inputs from both eyes prune throughout the dLGN during the first postnatal week, and pruning is largely complete by P9/10. Engulfment was analyzed throughout the dLGN.

(B) Engulfment of RGC inputs is significantly increased during peak pruning in the dLGN (P5). *$p < 0.001$ by one-way ANOVA, n = 3 mice/age.

(C) Engulfment in P5 dLGN occurs most significantly in synapse-enriched (contralateral and ipsilateral dLGN) versus nonsynaptic (optic tract) regions. *$p < 0.01$ by Student's t test, n = 3 P5 mice. All error bars represent SEM.

(D) Representative surface rendered microglia from P5 (fluorescent image is shown in Figure 1B), P9, and P30 mouse dLGN. Engulfment of RGC inputs occurs during peak pruning (P5) versus older ages (P9 and P30). Enlarged insets denoted with a black dotted line. Grid line increments = 5 μm.

See also Figure S2.

robust pruning (P5), engulfment was high (Figures 2B and 2Di). As few as 4 days later (P9), when much of the pruning is nearly complete, engulfment of RGC inputs was significantly reduced (Figures 2B and Dii). Thus, microglia-mediated engulfment of RGC inputs is temporally correlated with a period of robust synaptic pruning within the developing dLGN. Importantly, similar to P5 dLGN, microglia within the P9 dLGN still retained phagocytic capacity as assessed by morphology and CD68 expression (Figures S2C and S2D). These data suggest a more specific mechanism is driving engulfment specifically during the peak pruning period in the P5 dLGN.

Microglia-Mediated Engulfment of RGC Inputs Is Regulated by Neural Activity

Synaptic pruning is thought to result from competition between neighboring axons for postsynaptic territory based on differences in patterns or levels of activity (Hua and Smith, 2004; Katz and Shatz, 1996; Sanes and Lichtman, 1999). In the dLGN, it is thought that RGC inputs compete for territory such that those inputs which are less active or "weaker" are pruned and lose territory as compared to those inputs that are "stronger" or more active, which elaborate and strengthen (Del Rio and Feller, 2006; Dhande et al., 2011; Huberman et al., 2008; Penn et al., 1998; Shatz, 1990; Torborg and Feller, 2005). This competition can occur between inputs from the same eye as well as between inputs from both eyes (Chen and Regehr, 2000; Hooks and Chen, 2006; Jaubert-Miazza et al., 2005; Ziburkus and Guido, 2006). To determine whether microglia-mediated engulfment of RGC inputs is regulated by neural activity, P4 CX3CR1+/EGFP mice were injected with TTX (0.5 μM) to block RGC activity or forskolin to increase activity (10 mM) (Cook et al., 1999; Dunn et al., 2006; Shatz and Stryker, 1988; Stellwagen and Shatz, 2002; Stellwagen et al., 1999) in the left eye and vehicle (saline or DMSO, respectively) in the right eye. In order to distinguish inputs from each eye, RGC inputs were anterogradely labeled with CTB-594 (TTX or forskolin inputs) and CTB 647 (vehicle inputs) following drug injection (Figures 3A and 3D). At P5, mice were sacrificed and engulfment was assessed in a region with a similar proportion of ipsilateral and contralateral eye inputs.

When mice were injected with TTX and vehicle in the left and right eyes, respectively, microglia phagocytosed significantly more inputs from the less active TTX-treated eye (CTB-594, red) as compared to the vehicle-treated eye (CTB-647, blue) (Figures 3B and 3C). Likewise, mice injected with forskolin and vehicle engulfed significantly more inputs from the vehicle-treated eye (CTB-647, blue) as compared to the more active forskolin-treated eye (CTB-594, red) (Figures 3E and 3F). Importantly, this effect occurred in the absence of any significant increase in RGC death (Figure S3). Taken together, these data

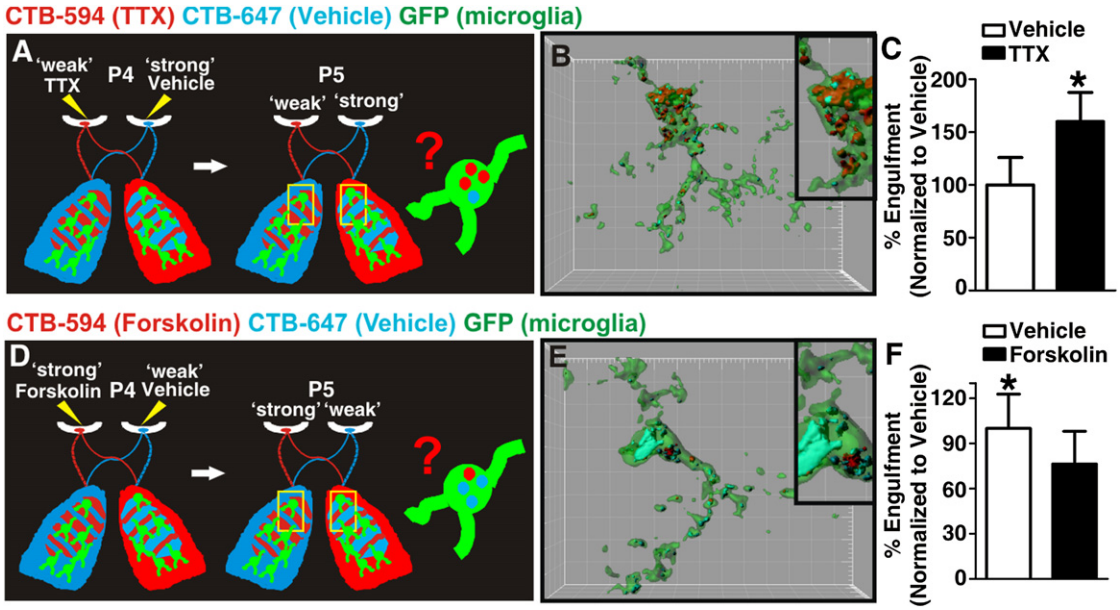

Figure 3. Microglia-Mediated Engulfment of RGC Inputs Is Regulated by Neural Activity

(A and D) Schematic of strategies used for assessing microglia engulfment following disruption of dLGN pruning by manipulation of neuronal activity.

(B) Representative P5 microglia (green) surface rendered from the border region of ipsilateral and contralateral projections in which left and right eyes were treated with TTX (red) and vehicle (blue), respectively. Inset is an enlarged region demonstrating the increase in engulfment of inputs from the "weaker," TTX-treated eye (red) as compared to those inputs derived from the "stronger" vehicle-treated eye (blue). Grid line increments = 5 μm.

(C) Significantly more TTX-treated inputs (black bar) are engulfed as compared to vehicle-treated inputs (white bar). *$p < 0.04$ by Student's t test, n = 4 mice/treatment.

(E) Representative P5 microglia (green) surface rendered from the border region of ipsilateral and contralateral projections in which left and right eyes were treated with forskolin (red) and vehicle (blue), respectively. Inset is an enlarged region demonstrating an increase in engulfment of inputs from the "weaker," vehicle-treated eye (blue) as compared to those inputs derived from the "stronger" forskolin-treated eye (red). Grid line increments = 5 μm.

(F) Significantly more vehicle-treated inputs (white bar) are engulfed as compared to forskolin-treated inputs (black bar) within the same dLGN. *$p < 0.04$ by Student's t test, n = 5 mice/treatment.

All error bars represent SEM. See also Figure S3.

demonstrate that microglia-mediated engulfment of RGC inputs is regulated by activity such that microglia preferentially engulf inputs from the "weaker" eye and suggest that microglia are active participants in synaptic pruning.

Microglia Engulf Presynaptic Elements Specific to RGCs

While it is clear that microglia engulf RGC inputs in a developmental and activity-dependent manner, it is unclear whether engulfed material is axonal and/or synaptic. Consistent with synaptic engulfment, significantly more RGC inputs were engulfed within synapse enriched regions of the P5 dLGN compared to a non-synaptic region, the optic tract (Figure 2C). To better determine the identity of engulfed material, electron microscopy was performed.

Microglia were identified by EM using criteria previously described including a small, irregular shaped nucleus containing substantial amounts of coarse chromatin and a cytoplasm rich in free ribosomes, vacuoles, and lysosomes (Mori and Leblond, 1969; Sturrock, 1981). Consistent with our confocal data, we observed several inclusions completely within the microglia cytoplasm including several double membrane-bound structures which contained 40 nm vesicles, data consistent with engulfment of presynaptic terminals (Figures 4A, 4B, and S4). In a few instances, structures reminiscent of juxtaposed pre- and postsynaptic structures were observed (Figure 4Aii).

To further confirm microglia-mediated phagocytosis of synaptic elements, immunohistochemical electron microscopy (immunoEM) for the microglia marker iba-1 was performed and quantified in the P5 dLGN (Figure 4C; Tremblay et al., 2010b). Consistent with EM data described above, we observed membrane-bound structures containing 40 nm presynaptic vesicles that were completely surrounded (Figure 4D) or enwrapped (Figure 4E) by DAB-positive microglial cytoplasm. To further support that microglia engulf material specific to presynaptic terminals, 40 nm vesicles were enriched in presynaptic terminals (Figures 4Bii and 4F) and very rarely visualized in cross or longitudinal sections of axons (Figure 4G). Indeed, presynaptic elements were observed within 35% of the microglia sampled (Figure 4I). Interestingly, several intact presynaptic terminals (Figure 4F) and all engulfed or enwrapped presynaptic inputs (Figures 4A, 4B, 4D, and 4E) lacked mitochondria, a characteristic feature of presynaptic terminals. Previous work has suggested that sensory deprivation or pharmacological blockade of neuronal activity (i.e., TTX) results in reduced mitochondria in presynaptic terminals known to undergo subsequent elimination (Hevner and Wong-Riley, 1993; Tieman, 1984). Thus, we

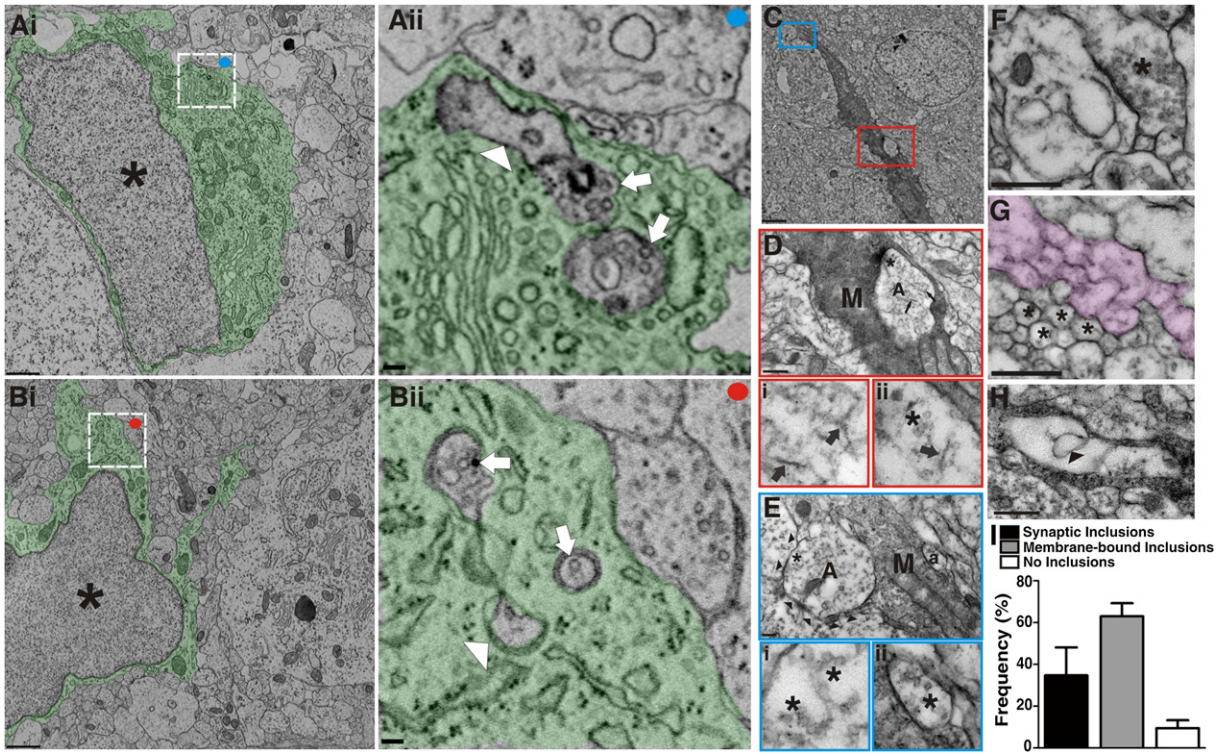

Figure 4. Microglia Engulf Preysnaptic Elements Undergoing Active Synaptic Pruning

(Ai and Bi) Low magnification EM of microglia. Asterisks denote the nucleus and the cytoplasm is pseudocolored green. Scale bar = 1 μm. (Aii and Bii) Magnified regions of Ai and Bi (white boxes) demonstrating membrane-bound elements engulfed by microglia. Arrows designate elements containing presynaptic machinery (40 nm vesicles). The arrowhead in (Aii) designates engulfed material resembling juxtaposed postsynaptic elements. Scale bar = 100 nm.

(C) Low-magnification EM of a microglia immunolabeled for iba-1 in P5 dLGN (DAB-positive cell). Red and blue boxes indicate enlarged regions in (D) and (E), respectively. Scale bar = 2 μm.

(D) RGC input (A) localized within the iba-1-positive microglia (M). Within the engulfed input, neurofilaments (arrows, enlarged in Di and Dii) and 40 nm vesicles (asterisks, enlarged in Dii) are indicative of presynaptic machinery. Scale bar = 500 nm.

(E) RGC input (A) enwrapped by a microglial process (M; arrowheads denote microglial process). 40 nm vesicles are also visible (asterisks, enlarged region in Ei). Another presynaptic element (a) containing 40 nm vesicles is surrounded by microglia cytoplasm (enlarged region in Eii). Scale bars = 100 nm.

(F) An intact excitatory synapse in P5 dLGN in which the presynaptic terminal (asterisk) contains 40 nm vesicles. Scale bar = 500 nm.

(G) Cross (asterisks) or longitudinal sections (pseudocolor) through axons are relatively void of vesicles. Scale bars = 500 nm.

(H) A membrane-bound structure (arrowhead) completely within a microglial lysosome. Scale bar = 500 nm.

(I) The frequency at which engulfed material was observed in microglia from P5 dLGN, n = 20 cells.

Error bars represent SEM. See also Figure S4.

suspect that these terminals deficient in mitochondria may be those destined for elimination.

In addition to presynaptic element engulfment, 63% of the sampled cells contained structurally unidentifiable membrane-bound inclusions within microglial lysosomal compartments (Figure 4H). We suspect that this membranous cellular material is synaptic material rapidly degraded in lysosomal compartments, thereby rendering it undistinguishable by ultrastructure. Unlike presynaptic elements, engulfed material resembling postsynaptic elements was very rarely observed (Figure 4Aii). However, rapid degradation of structural elements may preclude visualization of the postsynaptic density. Importantly, there were rare instances in which no engulfed material was observed within microglia (Figure 4I; no inclusions, 10% of sampled cells).

To directly address whether microglia are engulfing RGC presynaptic terminals, immunohistochemistry in P5 dLGN for presynaptic machinery specific to RGCs (i.e., VGlut2) followed by high resolution imaging was performed. 3D structural illumination microscopy (3D-SIM), a technique enabling 2X the resolution of light microscopy (Gustafsson, 2000), was used to assess the P5 dLGN of CX3CR1+/EGFP mice immunolabeled for VGlut2. 3D-SIM data revealed VGlut2 immunoreactivity within the EGFP-positive cytoplasm of microglial cells (Figures 5A–5D). Consistent with previous confocal and ultrastructural data (Figures 1, 2, 3, and 4), these data suggest that microglia are engulfing RGC presynaptic terminals.

To further confirm that microglia were engulfing RGC presynaptic terminals, double immunoEM in P5 dLGN for iba-1 (DAB) and a presynaptic marker specific to RGC terminals, VGlut2 (immunogold; Figures 5E–5G) was performed. Consistent with 3D-SIM data previously described, we observed immunogold labeling for VGlut2 within the microglia cytoplasm and lysosomes

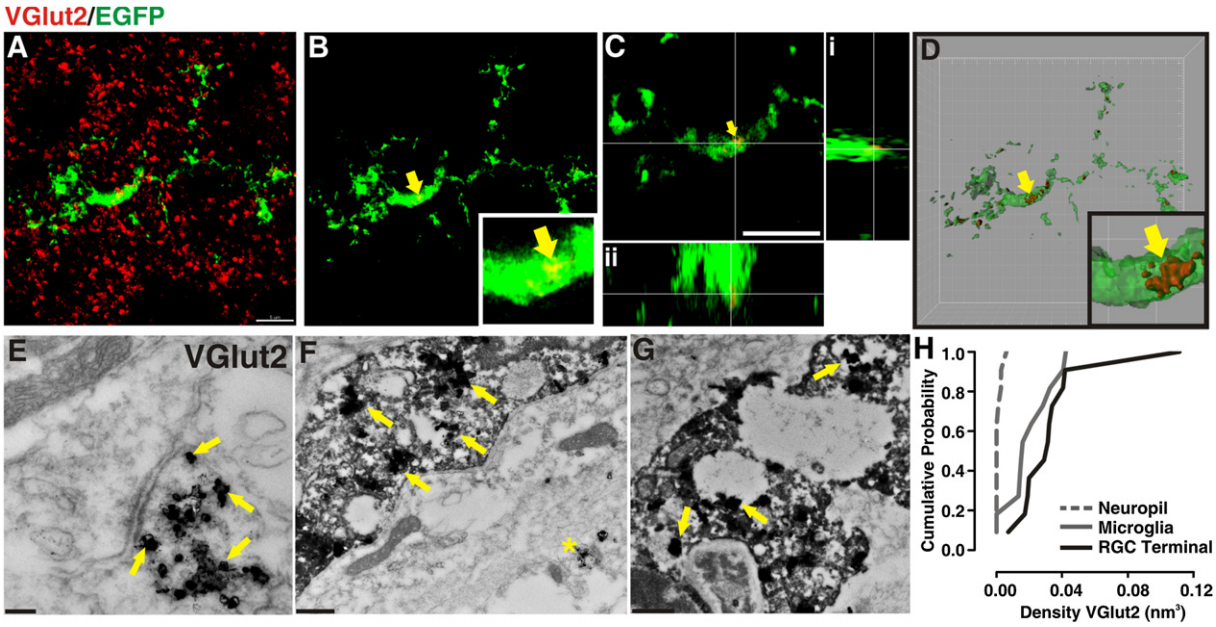

Figure 5. Microglia Engulf Presynaptic Terminals Specific to RGCs

(A–D) 3D-SIM in P5 CX3CR1+/EGFP dLGN in which microglia are labeled with EGFP (green) and RGC presynaptic terminals are immunolabeled with anti-VGlut2 (red). (A) Maximum intensity projection (MIP) of microglia and VGlut2 immunostaining in P5 dLGN. (B) MIP in which all VGlut2 fluorescence (red) that is not within the microglia (green) has been subtracted. Yellow arrow designates examples of engulfed VGlut2-positive elements, enlarged in inset. (C and D) Orthogonal views (C) and surface rendering (D) of region in (B) (yellow arrow and inset). (A–D) Scale bar = 5 μm. (D) Grid line increments = 2 μm.

(E–G) Double immunoEM in P5 dLGN for iba-1 (DAB) and VGlut2 (immunogold). (E) RGC presynaptic terminals are enriched with VGlut2 immunoreactivity (immunogold, yellow arrows). (F and G) Similar to RGC terminals (E), microglial cytoplasm (DAB), and lysosomes contain VGlut2 immunogold labeling (yellow arrows). Asterisk in (F) denotes a VGlut2-positive presynaptic terminal within the same field of view as the microglia. Scale bars = 100nm.

(H) Cumulative probability demonstrates that there is increased probability of VGlut2 localization to a RGC terminal (black solid line) or microglia (gray solid line) versus random occurrence throughout the neuropil (gray dotted line). For each structure, n = 10.

(Figures 5F, and 5G). Because immunogold was overexposed in order to gain contrast against the DAB reactivity, vesicle membranes surrounding the VGlut2 labeling were not observed within intact presynaptic terminals (Figure 5E) or microglia (Figures 5F and 5G). In addition, cumulative probability calculations demonstrated an increased probability of VGlut2 localized to an RGC terminal or microglia as compared to random immunoreactivity throughout the neuropil (Figure 5H). Similar to results from confocal microscopy experiments (Figures 1, 2, and 3), these ultrastructural data reveal that microglia engulf presynaptic terminals specific to RGCs.

Deletion of CR3/C3-Dependent Phagocytic Signaling Decreases the Capacity of Microglia to Engulf RGC Inputs

What molecular mechanism(s) underlies microglia-mediated engulfment of synaptic inputs? In the peripheral immune system, phagocytic cells can interact with several different immune-related signaling pathways to mediate clearance of cellular material. Included among these pathways are proteins belonging to the classical complement cascade, which bind surface receptors expressed by phagocytic cells. Given previous work demonstrating that complement component C3 is enriched at synapses and is necessary for pruning of retinogeniculate synapses (Stevens et al., 2007), we hypothesized that C3 ligand-receptor signaling may be one molecular mechanism by which microglia interact with and engulf RGC synaptic inputs.

Consistent with this hypothesis, CR3, a high-affinity receptor for activated C3 (Akiyama and McGeer, 1990; Perry et al., 1985), was specifically upregulated in microglia in the P5 dLGN and downregulated at later developmental time points (Figure 6A). Importantly, other cell types known to express the surface receptor CR3 and/or have phagocytic capacity (i.e., infiltrating monocytes, macrophages, etc.) were completely absent from the P5 dLGN and surrounding brain tissue (Figure S5; Akiyama and McGeer, 1990; Perry et al., 1985). As a result, in the context of the P5 brain, genetic manipulation of CR3 is specific to microglial cells. Similar to CR3 and consistent with our previous work, immunohistochemistry for CR3 ligand, C3, was enriched in synaptic regions of P5 dLGN and downregulated by P9, an age when pruning is largely complete (Figure 6B; Stevens et al., 2007). These data demonstrate that CR3 and its ligand, C3, are expressed at an appropriate age and location to mediate RGC input engulfment.

Using the in vivo phagocytosis assay previously described (Figure 2), engulfment was assessed in P5 mice lacking functional CR3 (CR3 KO) due to a genetic deletion of the alpha subunit, *CD11b* (Figure S5B; Coxon et al., 1996) or mice deficient in CR3 ligand, C3 (C3 KO) (Figure S5A). Microglia sampled from P5 CR3 or C3 KO mice had a statistically significant decrease in

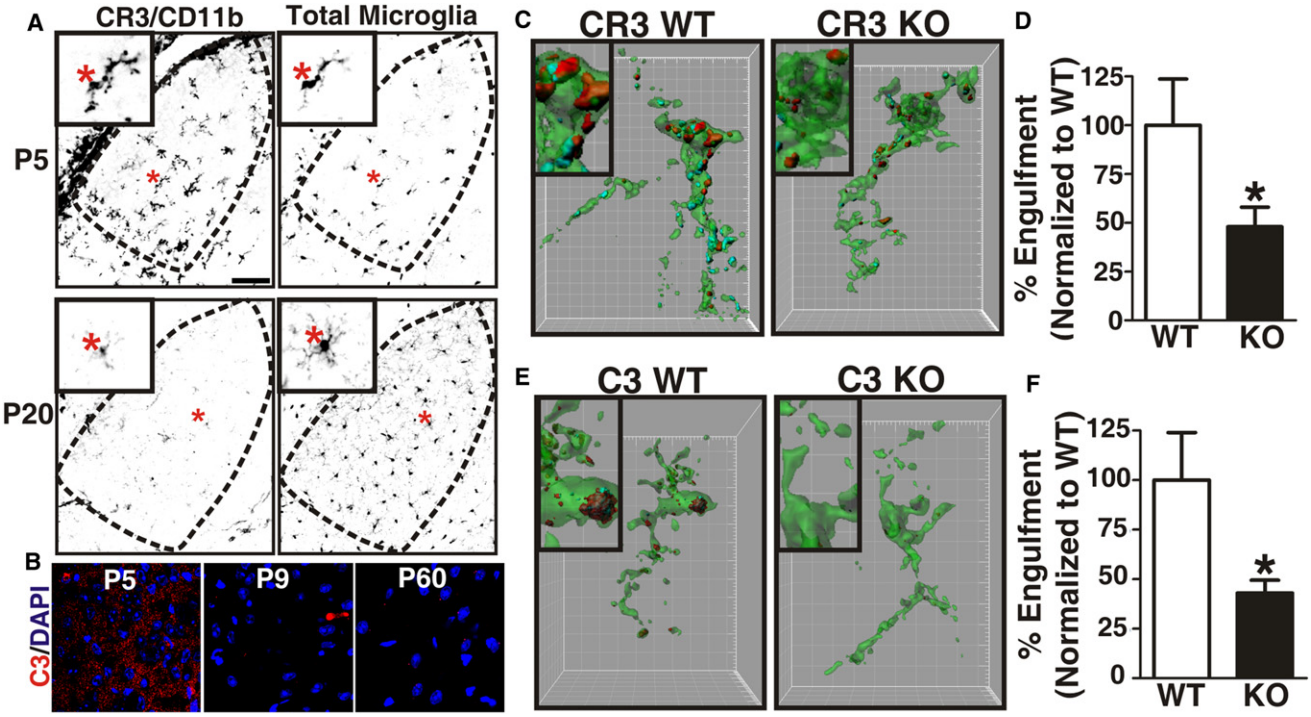

Figure 6. CR3/C3-Dependent Signaling Regulates Engulfment of Synaptic Inputs by Microglia

(A) Immunohistochemistry for the alpha subunit of CR3 (CD11b) reveals that microglia express high levels of CR3/CD11b (left column) in the P5 dLGN (top panels) versus older ages (P20, bottom panels). Total microglia are visualized with GFP (CX3CR1+/EGFP, right column). Insets are magnified regions (red asterisks). Scale bar = 100 μm.

(B) Immunohistochemistry in the developing dLGN for C3 (red). A single plane confocal image reveals that C3 levels are increased in the P5 dLGN versus older ages (P9, P60). Scale bar = 10 μm.

(C and E) Representative surface rendered microglia (green) from P5 dLGN of WT (left) or KO (right) littermates in which RGC inputs were labeled with CTB-594 (red, contralateral) and CTB-647 (blue, ipsilateral). Insets are enlarged regions demonstrating reduced RGC input engulfment (red and blue) in CR3 (C) and C3 (E) KO mice. Grid line increments = 5 μm.

(D and F) P5 CR3 KO (D) and C3 KO (F) mice (black bars) engulf significantly fewer RGC inputs as compared to WT littermates (white bars). All data are normalized to WT control values.

(D) *$p < 0.04$ by Student's t test, n = 3 mice/genotype. (E) *$p < 0.01$ Student's t test, n = 4 mice/genotype. All error bars represent SEM. See also Figure S5.

capacity to engulf RGC inputs as compared to WT littermate controls (Figures 6C–6F). Taken together, these data demonstrate that phagocytic signaling through CR3 and its ligand C3 is one molecular mechanism by which microglia engulf RGC inputs.

Disruption of CR3 Signaling in Microglia Results in Sustained Deficits in Structural Remodeling of RGC Inputs

During the first postnatal week, overlapping inputs from both eyes segregate into eye specific territories (i.e., eye-specific segregation), resulting in the termination of ipsilateral and contralateral inputs in distinct nonoverlapping domains in the mature dLGN (see Figure 2A; Godement et al., 1984; Guido, 2008; Huberman et al., 2008; Jaubert-Miazza et al., 2005; Sretavan and Shatz, 1986; Ziburkus and Guido, 2006). Consistent with our hypothesis that microglia play a role in synaptic pruning, C3 KO mice have previously been shown to have deficits in eye-specific segregation (Stevens et al., 2007). To determine whether microglia are mediators of C3-dependent synaptic refinement in the CNS, we quantified eye-specific segregation in CR3 KO mice. Ipsilateral and contralateral RGC inputs were labeled by intraocular injection of CTB-594 (red) and CTB-488 (green), respectively. Animals were subsequently sacrificed within 24 hr of the initial dye injection and overlap (yellow) between contralateral and ipsilateral RGC projection territories was quantified. In this experimental paradigm, an increase in the % overlap between the ipsilateral and contralateral projections within the dLGN is indicative of a deficit in synaptic pruning (Bjartmar et al., 2006; Huh et al., 2000; Pham et al., 2001; Ravary et al., 2003; Stevens et al., 2007).

Consistent with the hypothesis that microglia mediate complement-dependent synaptic pruning, a statistically significant increase in ipsilateral and contralateral input overlap was observed in P10 and P30 CR3 KOs as compared to WT littermate controls (Figures 7A–7C). This increase in overlap was attributed to a significantly broader ipsilateral projection territory (Figure 7D) and a small, but not significant, increase in the contralateral projection territory (Figure 7E). Furthermore, at higher magnification we detected aberrant ipsilateral and contralateral RGC inputs within the inappropriate monocular region (contralateral

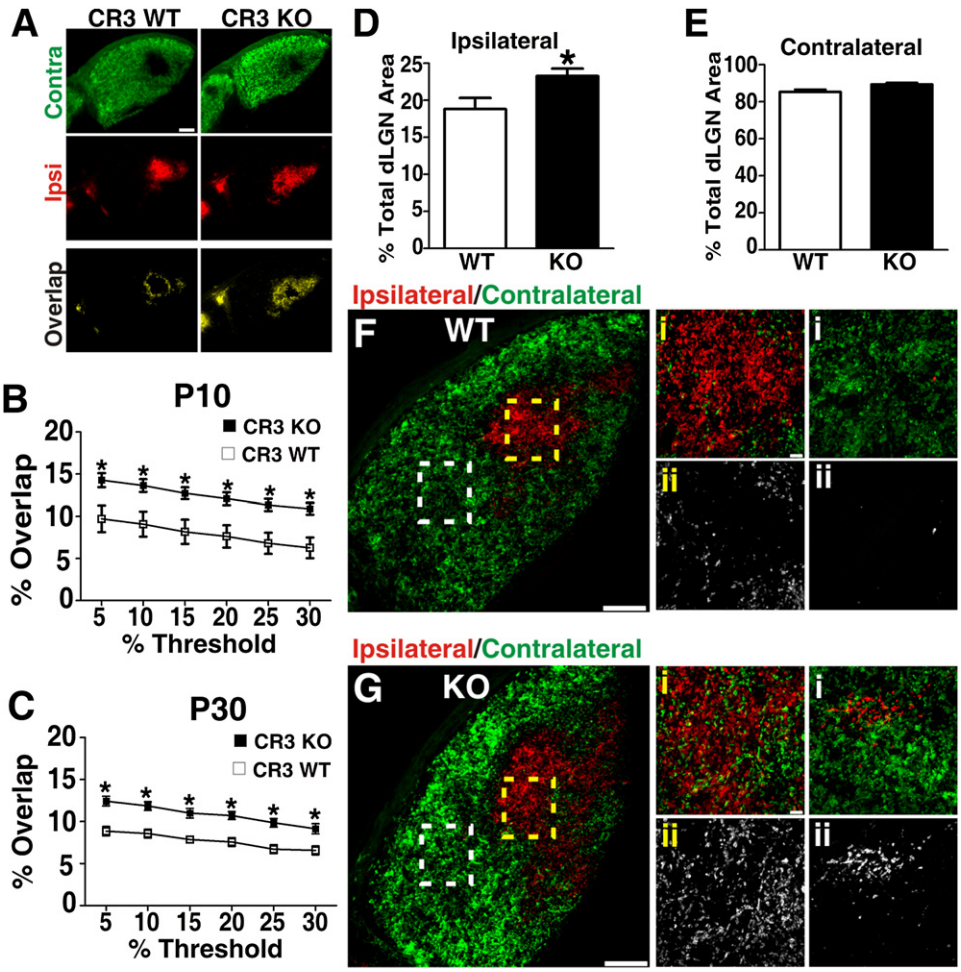

Figure 7. CR3 KO Mice Have Sustained Deficits in Eye-Specific Segregation

(A) Representative image of a P30 WT (left) demonstrates minimal overlap (yellow) between ipsilateral (red) and contralateral (green) RGC inputs. Indicative of a synaptic pruning deficit, CR3 KO mice (right) had increased overlap (yellow) of ipsilateral (red) and contralateral (green) RGC inputs. Scale bar = 100 μm.

(B and C) P10 (B) and P30 (C) CR3 KO mice had statistically significant, threshold-independent deficits in retinogeniculate pruning.

(D) The percentage of ipsilateral territory is significantly increased in P30 CR3 KO mice as compared to WT littermate controls.

(E) Although trending toward an increase, there is no statistically significant difference in percentage of contralateral territory.

(F and G) dLGN from P30 CR3 WT (F) or KO (G) mice, dotted line boxes in lower magnification image (left panels) correspond to ipsilateral region magnified in middle panels (yellow i–ii) or contralateral region magnified in far right panels (white i–ii). Bottom panels in (F) and (G) (ii) are contralateral (CTB-488, green, left panel) channel or ipsilateral (CTB-594, red, right panel) alone. (G) There were increased aberrant contralateral projections (middle panel; i, green, and ii) within the ipsilateral territory in P30 CR3 KO mice as compared to WT littermates (F, middle panel). Similarly, there were aberrant ipsilateral projections (right panel; i, red, and ii) within contralateral regions of the dLGN in CR3 KO mice as compared to WT littermates (F, right panel). Left panels, scale bar = 100 μm. Middle and right panels, scale bar = 10 μm.

(B and C) *$p < 0.0001$ by Student's t test, n = 6 (P10) or 4 (P30) mice/genotype. (D) *$p < 0.03$ by Student's t test, n = 4 mice/genotype. All error bars represent SEM. See also Figure S6.

and ipsilateral, respectively) in mature CR3 KO dLGN (P30; Figures 7F and 7G). In addition to genetic manipulation of CR3, microglia involvement in eye-specific segregation was further validated by manipulating microglia function pharmacologically using minocycline, an established inhibitor of microglial "activation" (Buller et al., 2009; Figures S6A–S6E). Similar to CR3 KO data, minocycline (P4–P8; 75 mg/kg) treatment during the peak of the pruning period resulted in reduced microglial phagocytic function (i.e., reduced RGC input engulfment) at P5 and a statistically significant deficit in eye-specific segregation at P10 (Figures S6C–S6E). Importantly, prior to any analyses we confirmed that any phenotype in KO or drug-treated mice was not due to differences in total RGC number within the retina and/or density of microglia within the dLGN (Figure S6F–S6K).

Taken together, disruption of microglia function by pharmacological (minocycline) or more specific genetic strategies (CR3 or C3 KOs) results in sustained deficits in eye-specific segregation within the dLGN. Furthermore, given that microglia are the only CNS cell that express CR3 in the postnatal dLGN, these data suggest that microglia are mediators of synaptic remodeling in

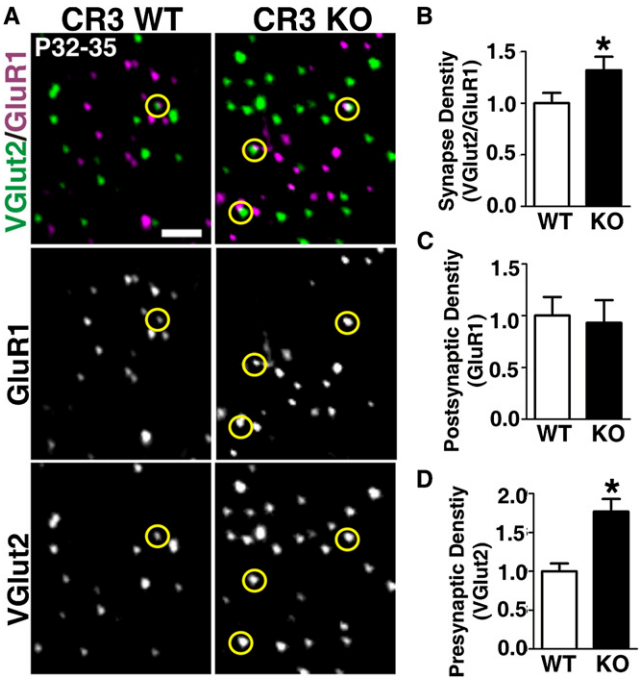

Figure 8. CR3 KO Mice Have a Sustained Increase in Synapse Density

(A) Single plane array tomography images for VGlut2 (green) to label RGC terminals and GluR1 (purple) to label postsynaptic excitatory sites in P32–P35 dLGN of CR3 KO (right) and WT littermate controls (left). Yellow circles indicate synapses defined by VGlut2 and GluR1 immunoreactivity. Scale bar = 2 μm. (B–D) Quantification of retinogeniculate synapse (B, VGlut2/GluR1-positive), postsynaptic (C, GluR1), and presynaptic/RGC terminal (D, VGlut2) density indicates that there is a statistically significant increase in retinogeniculate synapse density and total RGC terminal density in CR3 KOs as compared to WT littermates. *$p < 0.03$ Man-Whitney U test, $n = 3$ mice/genotype. Error bars represent SEM. See also Figure S7.

the retinogeniculate system and represent a key cellular mechanism underlying complement-dependent synaptic pruning (Stevens et al., 2007).

Disruption in CR3/C3-Dependent Signaling in Microglia Results in Sustained Deficits in Synaptic Connectivity

If CR3/C3-dependent signaling in microglia is a mechanism underlying developmental synaptic pruning, then a sustained increase in synapse density would be expected in the absence of these molecules. To test this possibility, retinogeniculate synapse density was quantified in adult CR3 KOs (P32–P35) using array tomography (AT), a powerful tool for high resolution imaging and quantification of synaptic density in vivo (Greer et al., 2010; Margolis et al., 2010; Micheva and Smith, 2007; Ross et al., 2010). RGC presynaptic terminals within the dLGN were labeled with an antibody directed against VGlut2 and postsynaptic excitatory sites were labeled with anti-GluR1. As suggested by the eye-specific segregation assay, there was a statistically significant increase (1.3-fold increase) in RGC synapse density (i.e., juxtaposed GluR1 and VGlut2 puncta) in adult CR3 KOs as compared to WT littermates (Figures 8A and 8B). Consistent with our previously published work (Stevens et al., 2007), adult C3 KO mice had an identical 1.3-fold increase in VGlut2-containing synapses as compared to WT littermate controls (Figure S7). Interestingly, there was also a significant increase in the density of total (both synapse associated and nonassociated) VGlut2-positive puncta in CR3 KOs (1.8-fold increase) as compared to WT littermates (Figure 8D). We hypothesize that these excess VGlut2-positive puncta represent residual immature synapses as well as retracted or unopposed immature presynaptic terminals that were not eliminated by phagocytic microglia. Taken together, these data implicate CR3/C3 signaling as a mechanism regulating synaptic connectivity.

Because microglia are the only cell type within the P5 dLGN and surrounding brain tissue to express CR3 (Figures 6 and S5; Akiyama and McGeer, 1990), our data directly implicate microglia as mediators of anatomical pruning and identify CR3/C3-dependent signaling as an underlying molecular mechanism.

DISCUSSION

In this study, we demonstrate that microglia are mediators of synaptic pruning in the normal, developing brain and identify neural activity and CR3/C3-dependent signaling as underlying mechanisms. Specifically, we demonstrate that (1) microglia in the postnatal dLGN engulf RGC presynaptic terminals during active synaptic remodeling. (2) Engulfment of RGC inputs is regulated by neuronal activity. (3) Engulfment of RGC inputs is regulated by CR3/C3-dependent phagocytic signaling specific to microglia. (4) Genetic (CR3 and C3 KO) or pharmacological perturbations that disrupt microglia function result in deficits in structural remodeling of synapses. (5) Defects in synaptic circuitry are sustained into adulthood in CR3 and C3 KO mice. We propose a model in which neural activity and complement work cooperatively to mediate engulfment of RGC inputs, a process that may underlie synaptic pruning in the developing CNS (Figure S7).

Microglia Engulf RGC Presynaptic Inputs during Peak Synaptic Pruning

One question arising is whether engulfment of RGC inputs by microglia is an active process. Particularly during CNS disease, microglia are known scavengers that phagocytose cellular debris (Hanisch and Kettenmann, 2007; Napoli and Neumann, 2009; Ransohoff and Perry, 2009). Furthermore, glia are known to engulf axonal material during large-scale developmental pruning of axons in *Drosophila* and synaptic pruning at the mammalian neuromuscular junction (Bishop et al., 2004; Freeman, 2006; Rochefort et al., 2002). While our results do not rule out the possibility that axonal material may also be engulfed, our data suggest that microglia play an active role in the removal of transient, intact presynaptic elements. Indeed, in comparison to large-scale developmental axonal pruning, there is no evidence that local CNS synaptic pruning, such as in the case of the retinogeniculate system, involves classic axonal or synaptic degeneration (Dhande et al., 2011; Hahm et al., 1999; Snider et al., 1999; Sretavan and Shatz, 1984). Earlier EM work in the developing mammalian dLGN demonstrated that RGCs transiently synapse within the inappropriate region of the

dLGN (Campbell and Shatz, 1992; Campbell et al., 1984). These transient synapses contained presynaptic machinery including a high density of vesicles, but were subsequently eliminated by an undetermined mechanism. Given our high resolution light microscopy and ultrastructure data, we suggest that microglia are actively pruning these transient synaptic connections via a phagocytic mechanism (Figure S7).

We provide several lines of evidence implicating microglia in the local pruning of transient, intact retinogeniculate synapses in the absence of axon debris or degeneration. First, in experiments involving anterograde tracing of RGCs (engulfment and eye-segregation assays), intraocular injections of dye occur less than 24 hr prior to tissue harvesting and fixation. If neurons or axons were degenerating, we would not expect effective dye uptake and tracing of the entire RGC projection. Furthermore, previous work has demonstrated that RGC normal programmed cell death is essentially complete by P4/P5 (Farah and Easter, 2005). Taken together, any CTB labeling observed within the dLGN is, more likely, originating from a healthy RGC cell body and axon. Second, previous work using dye tracing or fluorescent protein to label small subsets of RGC afferents in the dLGN demonstrate that RGC axons and arbors within the dLGN undergoing active pruning remain intact and unfragmented (Dhande et al., 2011; Hahm et al., 1999; Snider et al., 1999; Sretavan and Shatz, 1984). Consistent with these data, our EM experiments demonstrated that engulfed material as well as surrounding dLGN neuropil did not appear to have classic signs of axonal or synaptic degeneration such as multilamellar bodies, electron-dense cytoplasm, lack of synaptic vesicles within presynaptic terminals, etc. (Hoopfer et al., 2006; Perry and O'Connor, 2010). Lastly, we observed sustained increases in the number of intact, structural synapses by eye specific segregation and array tomography analyses in mice with disrupted microglia function (C3 KO, CR3 KO, and minocycline-treated mice). If synapses degenerated prior to engulfment, we would not expect to observe increased numbers of healthy, intact synapses in KO mice. Taken together, our data suggest that engulfed presynaptic elements were healthy, intact, and specifically engulfed by microglia.

Engulfment of RGC Inputs by Microglia Is an Activity-Dependent Process

Previous work has demonstrated that microglia have the capacity to interact with synaptic elements in response to neurotransmitter release and/or sensory experience (Biber et al., 2007; Fontainhas et al., 2011; Nimmerjahn et al., 2005; Ransohoff and Perry, 2009; Tremblay et al., 2010a; Wake et al., 2009). Furthermore, microglia can contribute to synaptic plasticity in the adult CNS and, more recently, in the context of the normal developing hippocampus (Paolicelli et al., 2011; Pascual et al., 2012; Roumier et al., 2008). Our data provide insight into mechanisms by which microglia may interact with synapses and contribute to activity-dependent synaptic plasticity. When competition between inputs from the two eyes was enhanced by pharmacological manipulation (i.e., TTX or forskolin), we found that microglia preferentially engulfed inputs from the eye in which neuronal activity was decreased or "weaker." Although it is not yet known whether or how microglia target specific "weaker" synapses, these data are consistent with previous work demonstrating that such a competition results in decreased territory of the "weaker" inputs and increased territory of "stronger" inputs within the dLGN (Del Rio and Feller, 2006; Huberman et al., 2008; McLaughlin et al., 2003; Penn et al., 1998; Shatz, 1990; Shatz and Stryker, 1988; Stellwagen and Shatz, 2002; Stellwagen et al., 1999; Torborg and Feller, 2005).

In the retina, spontaneous, correlated neuronal activity from both eyes (i.e., retinal waves) drives the elimination of synapses and segregation of inputs into eye-specific territories in the dLGN (Del Rio and Feller, 2006; Feller, 1999; Huberman et al., 2008; McLaughlin et al., 2003; Penn et al., 1998; Stellwagen and Shatz, 2002; Torborg and Feller, 2005). Interestingly, complement and complement receptor-deficient mice have similar pruning deficits to mice in which this correlated firing has been disrupted (e.g., cAMP-analog injection, $\beta 2nAChR^{-/-}$ mice, etc.) (Stevens et al., 2007), suggesting the intriguing possibility that complement cascade activation and function is regulated by neural activity. Neural activity could also directly regulate microglia function (i.e., activation, recruitment, phagocytic capacity) through complement-independent mechanisms. Alternatively, neural activity may drive the elimination of synapses by other mechanisms which ultimately lead to complement activation and/or microglia-mediated engulfment. Future studies will aim to address how neural activity, complement, and microglia may interact to contribute to developmental synaptic pruning (Figure S7).

CR3/C3-Dependent Signaling: A molecular Pathway Underlying Microglia-Mediated Synaptic Pruning

Synaptic pruning likely involves several mechanisms that cooperatively interact to establish precise synaptic circuits. We suggest that microglia may be a common link and identify CR3/C3 signaling as one pathway underlying microglia-synapse interactions and microglia-dependent pruning in the developing CNS. One of the major questions raised by these findings is precisely how secreted complement proteins mediate the selective elimination of synapses by microglia. In the immune system, C3 is cleaved into an activated form, iC3b, which covalently binds to the surface of cells or debris and targets them for elimination by macrophages via specific phagocytic receptor signaling (e.g., CR3) (Lambris and Tsokos, 1986; van Lookeren Campagne et al., 2007). Similar to the immune system, we propose that activated C3 (iC3b/C3b) could selectively "tag" weak synapses (Figure S7). Consistent with C3 "tagging" subsets of RGC terminals, previous confocal analysis revealed colocalization of C3 with pre and postsynaptic markers in the developing dLGN (Stevens et al., 2007). Furthermore, mice deficient in CR3, C3, and C1q, the initiating protein of the classical complement cascade, exhibit strikingly similar defects in developmental synaptic pruning (Figures 7, 8, and S7). Alternatively, other complement-dependent and/or -independent mechanisms may be involved. For example, C3 could bind all synapses and only those synapses that are "stronger" or more active are selectively protected by membrane-bound complement regulatory molecules (Kim and Song, 2006; Song, 2006). In contrast, selective, activity-dependent elimination of synapses could be driven by a complement-independent mechanism which subsequently results in complement binding and/or microglia-mediated

engulfment. For example, MHC class I molecules, another class of immune molecules demonstrated to play a critical role in retinogeniculate pruning, have been shown to be activity dependent, localized to synapses, and colocalized with C1q leaving the possibility that MHC class I molecules may play an upstream role in microglia-mediated pruning of synapses (Corriveau et al., 1998; Datwani et al., 2009; Goddard et al., 2007; Huh et al., 2000).

While our data demonstrate that CR3/C3 signaling specific to microglia is involved in the pruning of developing circuits and suggest that engulfment is the underlying mechanism, CR3 and C3 may be acting through other pathways independent of phagocytosis or may be downstream of other signaling pathways to mediate pruning. In addition, engulfment deficits in CR3 and C3 KO mice were reduced to approximately 50% of WT littermate control values, suggesting that other complement receptor-dependent (e.g., CR4, CRig, etc.) and independent phagocytic mechanisms may also be involved. Future studies will aim to address whether and how specific synapses are eliminated by complement and other microglia-dependent mechanisms and how neural activity plays a role in this process.

Complement-Dependent Engulfment of Synaptic Inputs: A More Global Mechanism Underlying Remodeling of Neural Circuits in the Healthy and Diseased CNS?

Our data raise the question as to whether complement and/or microglia-dependent engulfment of synaptic inputs represents a more global mechanism underlying CNS neural circuit plasticity. While in at least one other developing system local axonal retraction and synapse elimination appear to occur independent of microglia (Cheng et al., 2010), recent work describes a role for microglia at developing hippocampal synapses (Paolicelli et al., 2011). In addition, in vivo imaging studies in the cortex revealed that microglia dynamics and interactions with neuronal compartments change in response to neural activity and experience (Davalos et al., 2005; Nimmerjahn et al., 2005; Tremblay et al., 2010a; Wake et al., 2009). While these studies describe microglia dynamics at synapses, a precise function and molecular mechanism(s) underlying microglia-synapse interactions in these brain regions was unknown. Our study provides mechanistic insight into the dynamic between microglia and developing synapses and provides complement-dependent signaling as a potential mechanism in other brain regions. Consistent with this idea, deficits in complement component C1q result in an increase in the number of presynaptic boutons and exuberant excitatory connectivity in the cortex (Chu et al., 2010). Future studies will aim to test the role of complement in microglia-synapse interactions in other CNS regions known to undergo activity-dependent synaptic remodeling.

In addition to relevance in global remodeling of circuits in the healthy brain, our findings have important implications for understanding mechanisms underlying synapse elimination in the diseased brain. Consistent with this idea, abnormal microglia function and complement cascade activation have been associated with neurodegeneration of the CNS (Alexander et al., 2008; Beggs and Salter, 2010; Rosen and Stevens, 2010; Schafer and Stevens, 2010; Stephan et al., 2012). Indeed, in a mouse model of glaucoma, a neurodegenerative disease associated with RGC loss and gliosis, C1q and C3 are highly upregulated and deposited on retinal synapses and C1q deficiency or microglial "inactivation" with minocycline provide significant neuroprotection (Howell et al., 2011; Steele et al., 2006; Stevens et al., 2007). In addition to diseases associated with neurodegeneration, recent data from genome-wide association studies and analyses of postmortem human brain tissue have suggested that microglia and/or the complement cascade may also be involved in the development and pathogenesis of neurodevelopmental and psychiatric disorders (e.g., autism, obsessive compulsive disorder, schizophrenia, etc.) (Chen et al., 2010; Håvik et al., 2011; Monji et al., 2009; Pardo et al., 2005; Vargas et al., 2005). Thus, an intriguing possibility remains that microglia and/or complement dysfunction may be directly involved in diseases associated with synapse loss, dysfunction, and/or development.

Together, our data offer insight into mechanisms underlying activity-dependent synaptic pruning in the developing CNS, provide a role for microglia in the healthy brain, and provide important mechanistic insight into microglia-synapse interactions in the healthy and diseased CNS.

EXPERIMENTAL PROCEDURES

Animals

All experiments were reviewed and overseen by the institutional animal use and care committee in accordance with all NIH guidelines for the humane treatment of animals. See Supplemental Experimental Procedures for details.

Engulfment Analysis

Mice, except tdTomato-expressing mice (CHX10-cre::tdTomato), received intraocular injections of anterograde tracers at P4. All mice were sacrificed at P5 and brains were 4% PFA fixed overnight (4°C). Only those brains with sufficient dye fills were analyzed (see Supplemental Experimental Procedures for details).

Intraocular Injection of TTX or Forskolin

P4 CX3CR1::EGFP heterozygotes were anesthetized with isoflurane and given an intraocular injection of drug (0.5 μM TTX or 10mM forskolin) and vehicle (saline or DMSO) into the left and right eyes, respectively. Injection volume was approximately 200 nl. Four to five hours after first injection, mice received a second intraocular injection of CTB 594 and 647 into the left and right eyes, respectively. Mice were sacrificed at P5 for analysis.

Electron Microscopy

EM was performed in collaboration with J. Lichtman laboratory. Tissue was prepared and imaged as previously described with minor modifications (Hayworth et al., 2006). For immunoEM, dLGN from postnatal mice were prepared and immunostained with rabbit anti-Iba-1 (Wako) as previously described (Tremblay et al., 2010b). See Supplemental Experimental Procedures for details.

Eye Segregation Analysis

Mice received intraocular injection of cholera toxin-β subunit (CTB) and were sacrificed the following day. Tissue was processed and analyzed as previously described (Jaubert-Miazza et al., 2005; Stevens et al., 2007). All analyses were performed blind with littermate controls.

Array Tomography

Array tomography was performed as previously described with minor modifications (Greer et al., 2010; Margolis et al., 2010; Micheva and Smith, 2007; Ross et al., 2010; Stevens et al., 2007). See Supplemental Experimental Procedures for details.

SUPPLEMENTAL INFORMATION

Supplemental Information includes seven figures, two movies, and Supplemental Experimental Procedures and can be found with this article online at doi:10.1016/j.neuron.2012.03.026.

ACKNOWLEDGMENTS

We thank C. Chen, B. Sabatini, M. Tessier-Lavigne, G. Corfas, X. He, Z. He, L. Benowitz, and A. Huberman for their helpful discussions and reading of this manuscript; J. Sanes for the advice regarding CHX10-tdTomato experiments; J. Lichtman and R. Schalek for the technical expertise regarding EM experiments; E. Polk for performing preliminary engulfment analysis experiments; the imaging core at Children's Hospital Boston including T. Hill and L. Bu for their technical support; the electron microscopy core at Harvard Medical School including L. Benecchi and M. Ericsson for their technical support; C. Heller for assistance in quantification of data. Work was supported by grants from the Smith Family Foundation (B.S.), Dana Foundation (B.S.), John Merck Scholars Program (B.S.), NINDS (RO1-NS-07100801; B.S.), NRSA (F32-NS-066698; D.P.S.), NIDA (RO1-DA-15043; B.A.B.), NIH (RO1-NS-045500; M.E.G.), NIH (RO1-NS-32151; R.M.R.), National MS Society (RG4550; R.M.R), NIH (P30-HD-18655; MRDDRC Imaging Core).

Accepted: March 8, 2012
Published: May 23, 2012

REFERENCES

Akiyama, H., and McGeer, P.L. (1990). Brain microglia constitutively express beta-2 integrins. J. Neuroimmunol. *30*, 81–93.

Alexander, J.J., Anderson, A.J., Barnum, S.R., Stevens, B., and Tenner, A.J. (2008). The complement cascade: Yin-Yang in neuroinflammation—neuro-protection and -degeneration. J. Neurochem. *107*, 1169–1187.

Beggs, S., and Salter, M.W. (2010). Microglia-neuronal signalling in neuropathic pain hypersensitivity 2.0. Curr. Opin. Neurobiol. *20*, 474–480.

Biber, K., Neumann, H., Inoue, K., and Boddeke, H.W. (2007). Neuronal 'On' and 'Off' signals control microglia. Trends Neurosci. *30*, 596–602.

Bishop, D.L., Misgeld, T., Walsh, M.K., Gan, W.B., and Lichtman, J.W. (2004). Axon branch removal at developing synapses by axosome shedding. Neuron *44*, 651–661.

Bjartmar, L., Huberman, A.D., Ullian, E.M., Rentería, R.C., Liu, X., Xu, W., Prezioso, J., Susman, M.W., Stellwagen, D., Stokes, C.C., et al. (2006). Neuronal pentraxins mediate synaptic refinement in the developing visual system. J. Neurosci. *26*, 6269–6281.

Buller, K.M., Carty, M.L., Reinebrant, H.E., and Wixey, J.A. (2009). Minocycline: a neuroprotective agent for hypoxic-ischemic brain injury in the neonate? J. Neurosci. Res. *87*, 599–608.

Campbell, G., and Shatz, C.J. (1992). Synapses formed by identified retinogeniculate axons during the segregation of eye input. J. Neurosci. *12*, 1847–1858.

Campbell, G., So, K.F., and Lieberman, A.R. (1984). Normal postnatal development of retinogeniculate axons and terminals and identification of inappropriately-located transient synapses: electron microscope studies of horseradish peroxidase-labelled retinal axons in the hamster. Neuroscience *13*, 743–759.

Cardona, A.E., Pioro, E.P., Sasse, M.E., Kostenko, V., Cardona, S.M., Dijkstra, I.M., Huang, D., Kidd, G., Dombrowski, S., Dutta, R., et al. (2006). Control of microglial neurotoxicity by the fractalkine receptor. Nat. Neurosci. *9*, 917–924.

Chen, C., and Regehr, W.G. (2000). Developmental remodeling of the retinogeniculate synapse. Neuron *28*, 955–966.

Chen, S.K., Tvrdik, P., Peden, E., Cho, S., Wu, S., Spangrude, G., and Capecchi, M.R. (2010). Hematopoietic origin of pathological grooming in Hoxb8 mutant mice. Cell *141*, 775–785.

Cheng, T.W., Liu, X.B., Faulkner, R.L., Stephan, A.H., Barres, B.A., Huberman, A.D., and Cheng, H.J. (2010). Emergence of lamina-specific retinal ganglion cell connectivity by axon arbor retraction and synapse elimination. J. Neurosci. *30*, 16376–16382.

Chu, Y., Jin, X., Parada, I., Pesic, A., Stevens, B., Barres, B., and Prince, D.A. (2010). Enhanced synaptic connectivity and epilepsy in C1q knockout mice. Proc. Natl. Acad. Sci. USA *107*, 7975–7980.

Cook, P.M., Prusky, G., and Ramoa, A.S. (1999). The role of spontaneous retinal activity before eye opening in the maturation of form and function in the retinogeniculate pathway of the ferret. Vis. Neurosci. *16*, 491–501.

Corriveau, R.A., Huh, G.S., and Shatz, C.J. (1998). Regulation of class I MHC gene expression in the developing and mature CNS by neural activity. Neuron *21*, 505–520.

Coxon, A., Rieu, P., Barkalow, F.J., Askari, S., Sharpe, A.H., von Andrian, U.H., Arnaout, M.A., and Mayadas, T.N. (1996). A novel role for the beta 2 integrin CD11b/CD18 in neutrophil apoptosis: a homeostatic mechanism in inflammation. Immunity *5*, 653–666.

Datwani, A., McConnell, M.J., Kanold, P.O., Micheva, K.D., Busse, B., Shamloo, M., Smith, S.J., and Shatz, C.J. (2009). Classical MHCI molecules regulate retinogeniculate refinement and limit ocular dominance plasticity. Neuron *64*, 463–470.

Davalos, D., Grutzendler, J., Yang, G., Kim, J.V., Zuo, Y., Jung, S., Littman, D.R., Dustin, M.L., and Gan, W.B. (2005). ATP mediates rapid microglial response to local brain injury in vivo. Nat. Neurosci. *8*, 752–758.

Del Rio, T., and Feller, M.B. (2006). Early retinal activity and visual circuit development. Neuron *52*, 221–222.

Deriy, L.V., Gomez, E.A., Zhang, G., Beacham, D.W., Hopson, J.A., Gallan, A.J., Shevchenko, P.D., Bindokas, V.P., and Nelson, D.J. (2009). Disease-causing mutations in the cystic fibrosis transmembrane conductance regulator determine the functional responses of alveolar macrophages. J. Biol. Chem. *284*, 35926–35938.

Dhande, O.S., Hua, E.W., Guh, E., Yeh, J., Bhatt, S., Zhang, Y., Ruthazer, E.S., Feller, M.B., and Crair, M.C. (2011). Development of single retinofugal axon arbors in normal and β2 knock-out mice. J. Neurosci. *31*, 3384–3399.

Dunn, T.A., Wang, C.T., Colicos, M.A., Zaccolo, M., DiPilato, L.M., Zhang, J., Tsien, R.Y., and Feller, M.B. (2006). Imaging of cAMP levels and protein kinase A activity reveals that retinal waves drive oscillations in second-messenger cascades. J. Neurosci. *26*, 12807–12815.

Farah, M.H., and Easter, S.S., Jr. (2005). Cell birth and death in the mouse retinal ganglion cell layer. J. Comp. Neurol. *489*, 120–134.

Feller, M.B. (1999). Spontaneous correlated activity in developing neural circuits. Neuron *22*, 653–656.

Fontainhas, A.M., Wang, M., Liang, K.J., Chen, S., Mettu, P., Damani, M., Fariss, R.N., Li, W., and Wong, W.T. (2011). Microglial morphology and dynamic behavior is regulated by ionotropic glutamatergic and GABAergic neurotransmission. PLoS ONE *6*, e15973.

Freeman, M.R. (2006). Sculpting the nervous system: glial control of neuronal development. Curr. Opin. Neurobiol. *16*, 119–125.

Goddard, C.A., Butts, D.A., and Shatz, C.J. (2007). Regulation of CNS synapses by neuronal MHC class I. Proc. Natl. Acad. Sci. USA *104*, 6828–6833.

Godement, P., Salaün, J., and Imbert, M. (1984). Prenatal and postnatal development of retinogeniculate and retinocollicular projections in the mouse. J. Comp. Neurol. *230*, 552–575.

Greer, P.L., Hanayama, R., Bloodgood, B.L., Mardinly, A.R., Lipton, D.M., Flavell, S.W., Kim, T.K., Griffith, E.C., Waldon, Z., Maehr, R., et al. (2010). The Angelman Syndrome protein Ube3A regulates synapse development by ubiquitinating arc. Cell *140*, 704–716.

Guido, W. (2008). Refinement of the retinogeniculate pathway. J. Physiol. *586*, 4357–4362.

Gustafsson, M.G. (2000). Surpassing the lateral resolution limit by a factor of two using structured illumination microscopy. J. Microsc. *198*, 82–87.

Hahm, J.O., Cramer, K.S., and Sur, M. (1999). Pattern formation by retinal afferents in the ferret lateral geniculate nucleus: developmental segregation

and the role of N-methyl-D-aspartate receptors. J. Comp. Neurol. *411*, 327–345.

Hanisch, U.K., and Kettenmann, H. (2007). Microglia: active sensor and versatile effector cells in the normal and pathologic brain. Nat. Neurosci. *10*, 1387–1394.

Håvik, B., Le Hellard, S., Rietschel, M., Lybæk, H., Djurovic, S., Mattheisen, M., Mühleisen, T.W., Degenhardt, F., Priebe, L., Maier, W., et al. (2011). The complement control-related genes CSMD1 and CSMD2 associate to schizophrenia. Biol. Psychiatry *70*, 35–42.

Hayworth, K.J., Kasthuri, N., Schalek, R., and Lichtman, J.W. (2006). Automating the collection of ultrathin serial sections for large volume TEM reconstructions. Microsc. Microanal. *12*, 86–87.

Hevner, R.F., and Wong-Riley, M.T. (1993). Mitochondrial and nuclear gene expression for cytochrome oxidase subunits are disproportionately regulated by functional activity in neurons. J. Neurosci. *13*, 1805–1819.

Hooks, B.M., and Chen, C. (2006). Distinct roles for spontaneous and visual activity in remodeling of the retinogeniculate synapse. Neuron *52*, 281–291.

Hoopfer, E.D., McLaughlin, T., Watts, R.J., Schuldiner, O., O'Leary, D.D., and Luo, L. (2006). Wlds protection distinguishes axon degeneration following injury from naturally occurring developmental pruning. Neuron *50*, 883–895.

Howell, G.R., Macalinao, D.G., Sousa, G.L., Walden, M., Soto, I., Kneeland, S.C., Barbay, J.M., King, B.L., Marchant, J.K., Hibbs, M., et al. (2011). Molecular clustering identifies complement and endothelin induction as early events in a mouse model of glaucoma. J. Clin. Invest. *121*, 1429–1444.

Hua, J.Y., and Smith, S.J. (2004). Neural activity and the dynamics of central nervous system development. Nat. Neurosci. *7*, 327–332.

Huberman, A.D., Feller, M.B., and Chapman, B. (2008). Mechanisms underlying development of visual maps and receptive fields. Annu. Rev. Neurosci. *31*, 479–509.

Huh, G.S., Boulanger, L.M., Du, H., Riquelme, P.A., Brotz, T.M., and Shatz, C.J. (2000). Functional requirement for class I MHC in CNS development and plasticity. Science *290*, 2155–2159.

Jaubert-Miazza, L., Green, E., Lo, F.S., Bui, K., Mills, J., and Guido, W. (2005). Structural and functional composition of the developing retinogeniculate pathway in the mouse. Vis. Neurosci. *22*, 661–676.

Jung, S., Aliberti, J., Graemmel, P., Sunshine, M.J., Kreutzberg, G.W., Sher, A., and Littman, D.R. (2000). Analysis of fractalkine receptor CX(3)CR1 function by targeted deletion and green fluorescent protein reporter gene insertion. Mol. Cell. Biol. *20*, 4106–4114.

Katz, L.C., and Shatz, C.J. (1996). Synaptic activity and the construction of cortical circuits. Science *274*, 1133–1138.

Kim, D.D., and Song, W.C. (2006). Membrane complement regulatory proteins. Clin. Immunol. *118*, 127–136.

Kreutzberg, G.W. (1996). Microglia: a sensor for pathological events in the CNS. Trends Neurosci. *19*, 312–318.

Lambris, J.D., and Tsokos, G.C. (1986). The biology and pathophysiology of complement receptors. Anticancer Res. *6* (3 Pt B), 515–523.

Lynch, M.A. (2009). The multifaceted profile of activated microglia. Mol. Neurobiol. *40*, 139–156.

Margolis, S.S., Salogiannis, J., Lipton, D.M., Mandel-Brehm, C., Wills, Z.P., Mardinly, A.R., Hu, L., Greer, P.L., Bikoff, J.B., Ho, H.Y., et al. (2010). EphB-mediated degradation of the RhoA GEF Ephexin5 relieves a developmental brake on excitatory synapse formation. Cell *143*, 442–455.

McLaughlin, T., Torborg, C.L., Feller, M.B., and O'Leary, D.D. (2003). Retinotopic map refinement requires spontaneous retinal waves during a brief critical period of development. Neuron *40*, 1147–1160.

Micheva, K.D., and Smith, S.J. (2007). Array tomography: a new tool for imaging the molecular architecture and ultrastructure of neural circuits. Neuron *55*, 25–36.

Miksa, M., Komura, H., Wu, R., Shah, K.G., and Wang, P. (2009). A novel method to determine the engulfment of apoptotic cells by macrophages using pHrodo succinimidyl ester. J. Immunol. Methods *342*, 71–77.

Monji, A., Kato, T., and Kanba, S. (2009). Cytokines and schizophrenia: microglia hypothesis of schizophrenia. Psychiatry Clin. Neurosci. *63*, 257–265.

Mori, S., and Leblond, C.P. (1969). Identification of microglia in light and electron microscopy. J. Comp. Neurol. *135*, 57–80.

Napoli, I., and Neumann, H. (2009). Microglial clearance function in health and disease. Neuroscience *158*, 1030–1038.

Nimmerjahn, A., Kirchhoff, F., and Helmchen, F. (2005). Resting microglial cells are highly dynamic surveillants of brain parenchyma in vivo. Science *308*, 1314–1318.

Paolicelli, R.C., Bolasco, G., Pagani, F., Maggi, L., Scianni, M., Panzanelli, P., Giustetto, M., Ferreira, T.A., Guiducci, E., Dumas, L., et al. (2011). Synaptic pruning by microglia is necessary for normal brain development. Science *333*, 1456–1458.

Pardo, C.A., Vargas, D.L., and Zimmerman, A.W. (2005). Immunity, neuroglia and neuroinflammation in autism. Int. Rev. Psychiatry *17*, 485–495.

Pascual, O., Ben Achour, S., Rostaing, P., Triller, A., and Bessis, A. (2012). Microglia activation triggers astrocyte-mediated modulation of excitatory neurotransmission. Proc. Natl. Acad. Sci. USA *109*, E197–E205. Published online December 13, 2011. 10.1073/pnas.1111098109.

Penn, A.A., Riquelme, P.A., Feller, M.B., and Shatz, C.J. (1998). Competition in retinogeniculate patterning driven by spontaneous activity. Science *279*, 2108–2112.

Perry, V.H., and O'Connor, V. (2010). The role of microglia in synaptic stripping and synaptic degeneration: a revised perspective. ASN Neuro. *2*, e00047. 10.1042/AN20100024.

Perry, V.H., Hume, D.A., and Gordon, S. (1985). Immunohistochemical localization of macrophages and microglia in the adult and developing mouse brain. Neuroscience *15*, 313–326.

Pham, T.A., Rubenstein, J.L., Silva, A.J., Storm, D.R., and Stryker, M.P. (2001). The CRE/CREB pathway is transiently expressed in thalamic circuit development and contributes to refinement of retinogeniculate axons. Neuron *31*, 409–420.

Ransohoff, R.M., and Perry, V.H. (2009). Microglial physiology: unique stimuli, specialized responses. Annu. Rev. Immunol. *27*, 119–145.

Ravary, A., Muzerelle, A., Hervé, D., Pascoli, V., Ba-Charvet, K.N., Girault, J.A., Welker, E., and Gaspar, P. (2003). Adenylate cyclase 1 as a key actor in the refinement of retinal projection maps. J. Neurosci. *23*, 2228–2238.

Rochefort, N., Quenech'du, N., Watroba, L., Mallat, M., Giaume, C., and Milleret, C. (2002). Microglia and astrocytes may participate in the shaping of visual callosal projections during postnatal development. J. Physiol. Paris *96*, 183–192.

Rosen, A.M., and Stevens, B. (2010). The role of the classical complement cascade in synapse loss during development and glaucoma. Adv. Exp. Med. Biol. *703*, 75–93.

Ross, S.E., Mardinly, A.R., McCord, A.E., Zurawski, J., Cohen, S., Jung, C., Hu, L., Mok, S.I., Shah, A., Savner, E.M., et al. (2010). Loss of inhibitory interneurons in the dorsal spinal cord and elevated itch in Bhlhb5 mutant mice. Neuron *65*, 886–898.

Roumier, A., Pascual, O., Béchade, C., Wakselman, S., Poncer, J.C., Réal, E., Triller, A., and Bessis, A. (2008). Prenatal activation of microglia induces delayed impairment of glutamatergic synaptic function. PLoS ONE *3*, e2595.

Saederup, N., Cardona, A.E., Croft, K., Mizutani, M., Cotleur, A.C., Tsou, C.L., Ransohoff, R.M., and Charo, I.F. (2010). Selective chemokine receptor usage by central nervous system myeloid cells in CCR2-red fluorescent protein knock-in mice. PLoS ONE *5*, e13693.

Sanes, J.R., and Lichtman, J.W. (1999). Development of the vertebrate neuromuscular junction. Annu. Rev. Neurosci. *22*, 389–442.

Schafer, D.P., and Stevens, B. (2010). Synapse elimination during development and disease: immune molecules take centre stage. Biochem. Soc. Trans. *38*, 476–481.

Schafer, D.P., Lehrman, E.K., and Stevens, B. (2012). The "quad-partite" synapse: microglia-synapse interactions in the developing and mature CNS. Glia, in press.

Shatz, C.J. (1990). Competitive interactions between retinal ganglion cells during prenatal development. J. Neurobiol. *21*, 197–211.

Shatz, C.J., and Kirkwood, P.A. (1984). Prenatal development of functional connections in the cat's retinogeniculate pathway. J. Neurosci. *4*, 1378–1397.

Shatz, C.J., and Stryker, M.P. (1988). Prenatal tetrodotoxin infusion blocks segregation of retinogeniculate afferents. Science *242*, 87–89.

Snider, C.J., Dehay, C., Berland, M., Kennedy, H., and Chalupa, L.M. (1999). Prenatal development of retinogeniculate axons in the macaque monkey during segregation of binocular inputs. J. Neurosci. *19*, 220–228.

Song, W.C. (2006). Complement regulatory proteins and autoimmunity. Autoimmunity *39*, 403–410.

Sretavan, D., and Shatz, C.J. (1984). Prenatal development of individual retinogeniculate axons during the period of segregation. Nature *308*, 845–848.

Sretavan, D.W., and Shatz, C.J. (1986). Prenatal development of retinal ganglion cell axons: segregation into eye-specific layers within the cat's lateral geniculate nucleus. J. Neurosci. *6*, 234–251.

Steele, M.R., Inman, D.M., Calkins, D.J., Horner, P.J., and Vetter, M.L. (2006). Microarray analysis of retinal gene expression in the DBA/2J model of glaucoma. Invest. Ophthalmol. Vis. Sci. *47*, 977–985.

Stellwagen, D., and Shatz, C.J. (2002). An instructive role for retinal waves in the development of retinogeniculate connectivity. Neuron *33*, 357–367.

Stellwagen, D., Shatz, C.J., and Feller, M.B. (1999). Dynamics of retinal waves are controlled by cyclic AMP. Neuron *24*, 673–685.

Stephan, A., Barres, B.A., and Stevens, B. (2012). The complement system: an unexpected role in synaptic pruning during development and disease. Ann. Rev. Neurosci. *35*, 369–389.

Stevens, B., Allen, N.J., Vazquez, L.E., Howell, G.R., Christopherson, K.S., Nouri, N., Micheva, K.D., Mehalow, A.K., Huberman, A.D., Stafford, B., et al. (2007). The classical complement cascade mediates CNS synapse elimination. Cell *131*, 1164–1178.

Sturrock, R.R. (1981). Microglia in the prenatal mouse neostriatum and spinal cord. J. Anat. *133*, 499–512.

Tieman, S.B. (1984). Effects of monocular deprivation on geniculocortical synapses in the cat. J. Comp. Neurol. *222*, 166–176.

Torborg, C.L., and Feller, M.B. (2005). Spontaneous patterned retinal activity and the refinement of retinal projections. Prog. Neurobiol. *76*, 213–235.

Tremblay, M.E., Lowery, R.L., and Majewska, A.K. (2010a). Microglial interactions with synapses are modulated by visual experience. PLoS Biol. *8*, e1000527.

Tremblay, M.E., Riad, M., and Majewska, A. (2010b). Preparation of mouse brain tissue for immunoelectron microscopy. J. Vis. Exp. *20*, 2021. 10.3791/2021.

van Lookeren Campagne, M., Wiesmann, C., and Brown, E.J. (2007). Macrophage complement receptors and pathogen clearance. Cell. Microbiol. *9*, 2095–2102.

Vargas, D.L., Nascimbene, C., Krishnan, C., Zimmerman, A.W., and Pardo, C.A. (2005). Neuroglial activation and neuroinflammation in the brain of patients with autism. Ann. Neurol. *57*, 67–81.

Wake, H., Moorhouse, A.J., Jinno, S., Kohsaka, S., and Nabekura, J. (2009). Resting microglia directly monitor the functional state of synapses in vivo and determine the fate of ischemic terminals. J. Neurosci. *29*, 3974–3980.

Ziburkus, J., and Guido, W. (2006). Loss of binocular responses and reduced retinal convergence during the period of retinogeniculate axon segregation. J. Neurophysiol. *96*, 2775–2784.